Theoret. chim. Acta (Berl.) 28, 313–337 (1973)
© by Springer-Verlag 1973

Commentationes

A Semiempirical MO Study of the Electronic Structure and Excited States of the *Tris*(2,2′-Bipyridyl)Iron(II) and *Tris*(Glyoxal-*Bis*-N-Methylimine)Iron(II)Ions

Jan Blomquist

Institute of Physics, University of Stockholm, Vanadisvägen 9, 11346 Stockholm

Bengt Nordén

Dept. of Inorganic Chemistry, University of Lund, Box 740, 22007 Lund

Marianne Sundbom

Institute of Theoretical Physics, University of Stockholm, Vanadisvägen 9, 11346 Stockholm

Received May 23, 1972

A semi-empirical SCF–MO method, the PEEL method, has been applied in an investigation of the electronic structure and excited states of two iron compounds, $[Fe(II)\text{-}(GMI)_3]^{++}$ and $[Fe(II)\text{-}(bipy)_3]^{++}$.

The electronic absorption spectra have been recorded. The calculations show that it is necessary to account for the trigonal distortion and the covalency in order to explain these spectra quantitatively. Mössbauer measurements have also been performed. The calculated electronic population of the iron is in accord with Mössbauer isomer shift data, indicating that a realistic electron distribution has been obtained by the PEEL method.

Eine semiempirische SCF–MO-Methode, die PEEL-Methode, wurde zur Untersuchung der Elektronenstruktur sowie von angeregten Zuständen der beiden Eisenverbindungen $[Fe(II)\text{-}(GMI)_3]^{++}$ und $[Fe(II)\text{-}(bipy)_3]^{++}$ angewendet.

Die elektronischen Absorptionsspektren wurden aufgenommen. Die Berechnungen zeigen, daß die trigonale Verzerrung und die Kovalenz berücksichtigt werden müssen, um die Spektren quantitativ zu erklären. Mössbauer-Messungen wurden ebenfalls durchgeführt. Die berechnete Elektronenverteilung am Eisenatom ist in Übereinstimmung mit den Daten der Isomerenverschiebung der Mössbauer-Messungen, wodurch gezeigt wird, daß mit der PEEL-Methode eine realistische Elektronen-Verteilung erhalten wurde.

Une méthode SCF–MO semi-empirique, la méthode PEEL, a été appliquée à une étude de la structure électronique et des états excités de deux composés ferreux: $[Fe(II)\text{-}(bipy)_3]^{++}$ et $[Fe(II)\text{-}(GMI)_3]^{++}$. Les spectres d'absorption électronique ont été enregistrés. Les calculs montrent qu'il est nécessaire de rendre compte de la distorsion trigonale et de la covalence pour expliquer ces spectres quantitativement.

Des mesures de l'effet Mössbauer ont aussi été effectuées. La population électronique calculée du fer est en bon accord avec les données sur le déplacement isomérique de Mössbauer, ce qui indique que la méthode PEEL fournit une distribution électronique réaliste.

1. Introduction

To obtain an understanding of the activity of organic molecules and organometallic complexes it is necessary to know more about their electronic structure. The present investigation is part of a project whose object is molecular orbital (MO)

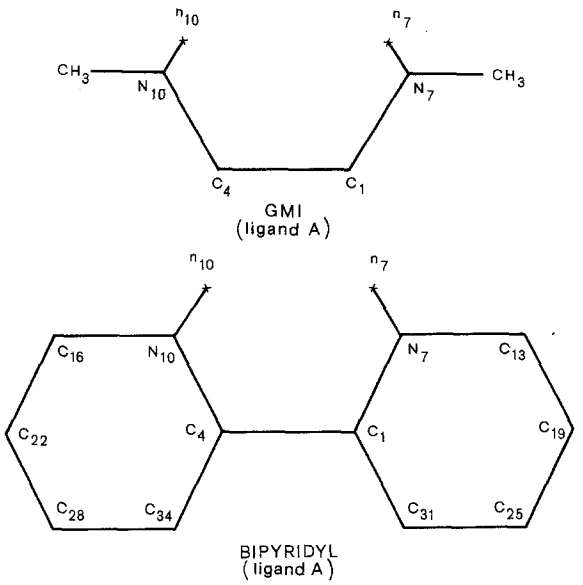

Fig. 1. The numbering of the AO's of GMI and bipyridyl. Cf. Fig. 2 and text

studies of molecules of biological interest. This study uses the PEEL method, an extended Pariser-Parr-Pople (PPP) method, that has proved to be successful in accounting for many different properties of large organic molecules [1–3] and organic copper complexes [4–7]. It was found worthwhile to extend the method to complexes of other transition elements. In the present paper the semiempirical parameters for iron complexes are presented.

The two propellershaped ions[1] $[Fe(II)\text{–}(bipy)_3]^{++}$ and $[Fe(II)\text{–}(GMI)_3]^{++}$ (bipy = 2,2′-bipyridyl; GMI = glyoxal-*bis*-N-methylimine) have been used as model compounds for the determination of semiempirical parameters describing the amount of bonding between iron and the nitrogen ligands. These molecules were chosen because they have been extensively investigated by experimental methods. The calculations have been performed for the right-handed optical isomers (cf. Figs. 1 and 2). The present MO study gives information about the electronic distribution within the complexes, especially the effective electronic population on the iron ion, from which a value of the total electronic density at the iron nucleus can be deduced and compared with the experimental value obtained from Mössbauer isomer shift data. Further, the study permits a discussion of the different types of transitions in the electronic spectra.

Reviews of previous theoretical investigations and experimental findings for $[Fe(II)\text{-}(bipy)_3]^{++}$ and $[Fe(II)\text{-}(GMI)_3]^{++}$ can be found in some recent publications [8, 9]. In most discussions of the electronic spectra of these compounds, octahedral symmetry (O_h) and crystal field theory have been considered adequate for the assignments. The results of the present investigation, however, show that it is necessary to account for the trigonal distortion and the covalency in order to

[1] In this paper the convention has been used that Fe(II) stands for ferrous iron, Fe^{2+}.

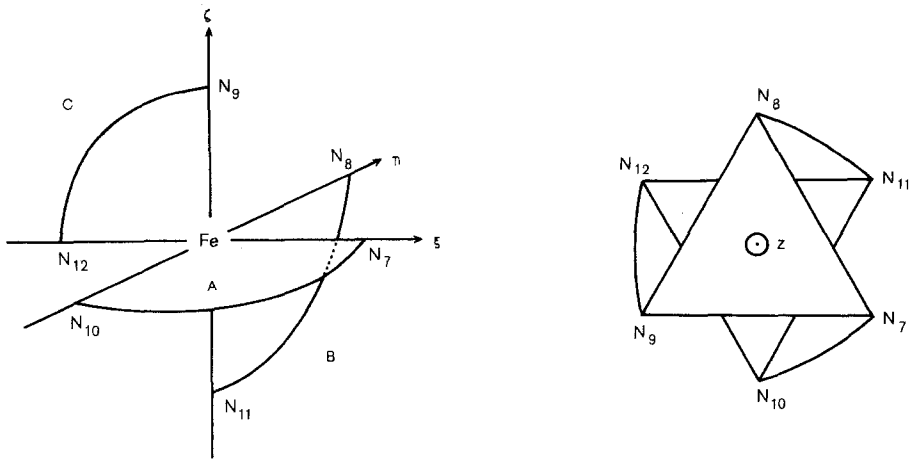

Fig. 2. The propellershaped structure of $[Fe(II)\text{–}(GMI)_3]^{++}$ and $[Fe(II)\text{–}(bipy)_3]^{++}$. *xyz* denotes the D_3 symmetry adapted right handed coordinate system with *z* as threefold axis and *x* through the twofold axis of ligand *A*. Cf. Fig. 1 and text

explain these spectra quantitatively. Day and Sanders [10, 11] discussed the CT band of the similar phenanthroline complex, using Hückel molecular orbitals and a simple treatment of CT states [12, 13]. In a more elaborate theoretical treatment of these molecules Ito, Tanaka, Hanazaki and Nagakura [14–16] were able to give a more quantitative discussion of the electronic transitions. They used an extension of the "molecules-in-molecule" method [13, 16] for their studies of metal complex ions, considered explicitly π orbitals of the ligands and *d* orbitals of the iron ion, and used locally excited ligand transitions together with electron transfer ($d \rightarrow \pi^*$) transitions in their CI-treatment. Thus their methods did not allow for a discussion of transitions of ($d \rightarrow d$) type.

In the present investigation 4*s* and 4*p* orbitals have been included, and the energy levels of excited states have been calculated by mixing all types of configurations obtained from single excitations. The theoretical model is discussed in Sections 3 and 4.

The electronic absorption spectra have been investigated experimentally and Mössbauer measurements have also been performed.

2. Experimental

Tris-(2,2'-bipyridyl) iron(II) sulphate was prepared according to a method of Jaeger and van Dijk [17]. The precipitate was washed with ether and dried over P_2O_5 for one week. It corresponded to a composition $Fe(bipy)_3 \cdot SO_4 \cdot 5H_2O$.

(*Analysis:* C 50.7, H 4.7, S 5, N 11.9; Calc. for $FeC_{30}N_6H_{24}SO_4 \cdot 5H_2$/: C 50.7, H 4.8, S 4.5, N 11.8.)

*Tris-(glyoxal-bis-*N*-methylimine) iron(II) iodide* was obtained in the way described by Krumholz [18] and dried over P_2O_5 for one week.

(*Analysis:* C 26.0, H 5.1, N 15.0; calculated for $FeC_{12}N_6H_{24}I_2$: C 25.6, H 4.3, N 14.9.)

The UV spectra in the range 15–54 kK were recorded on 10^{-4} M solutions (aqueous for the GMI complex, and methanolic for the bipyridyl complex) with a Cary 15 recording spectrophotometer. Spectrograde methanol was used without further purification. In the 10 kK range a Hitachi EPS-3T spectrophotometer was used on 0.3 M aqueous solutions. Concerning the iodide, it was carefully checked that no photolysis intervened. The UV spectrum could be exactly reproduced in several runs. The results are given in Tables 6, 7, 10 and 11 and Figs. 3 and 4.

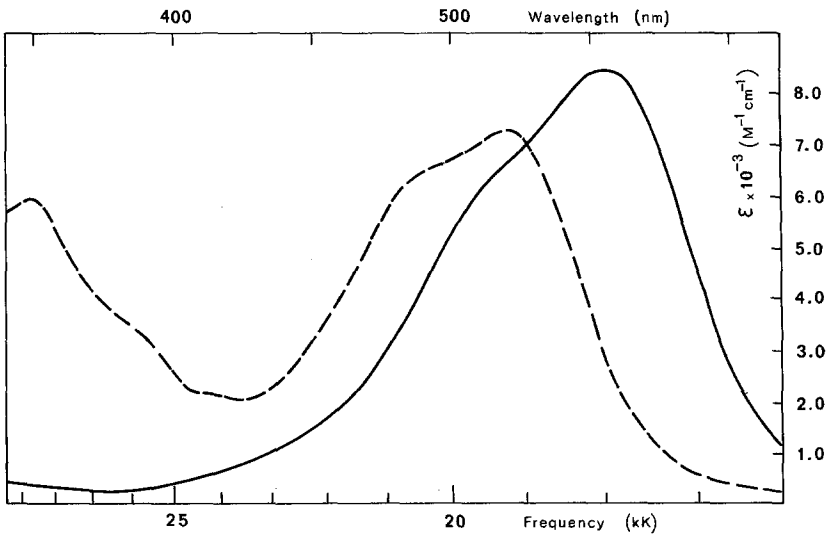

Fig. 3. The electronic absorption spectra of $[Fe(II)\text{–}(GMI)_3]$. I_2 in aqueous solution (———), and of $[Fe(II)\text{–}(bipy)_3] \cdot SO_4 \cdot 5H_2O$ in methanol (– – – –). The visible region

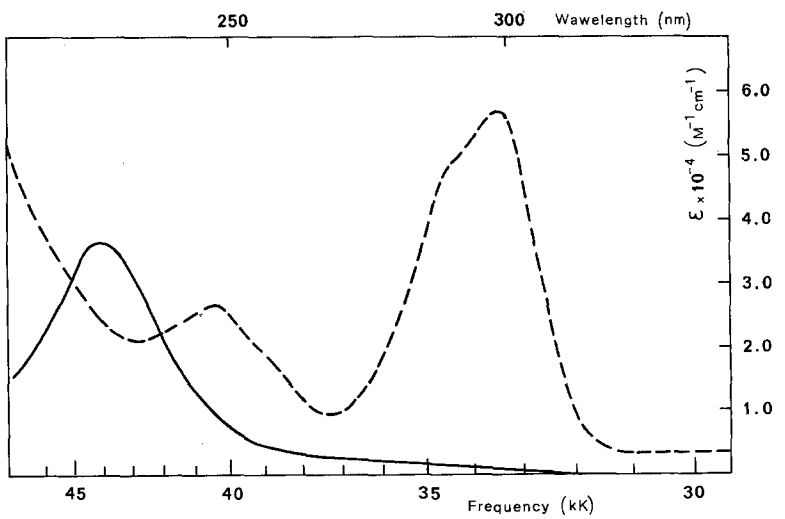

Fig. 4. The electronic absorption spectra of $[Fe(II)\text{–}(GMI)_3]$. I_2 in aqueous solution (———), and of $[Fe(II)\text{–}(bipy)_3] \cdot SO_4 \cdot 5H_2O$ in methanol (– – – –). The UV region

Mössbauer spectra were measured at room temperature with an electromechanical transducer of Kankeleit type in combination with an Intertechnique 400-channel analyser and a Hilger and Watts P 1028 scintillation detector. The source was 5 mC ^{57}Co in Pd foil kept at the same temperature as the absorber. The velocity was calibrated using the magnetic splitting of natural iron. The Mössbauer lines were fitted to Lorentzians by means of a least squares method. Also in this case the spectra were satisfactorily reproduced in several runs with different samples. The results are given in Table 5.

More details about the Mössbauer study can be found in Ref. [47].

3. Theoretical Model

In applying the methods of quantum chemistry to large molecular systems, approximations must be made to simplify the work required and reduce the amount of computertime utilized drastically. Roos and Skancke [19] suggested a new scheme for the evaluation of semiempirical parameters in a modified PPP-method for π systems. In order to allow for a systematic study of large organic molecules, this scheme has been extended. The method is now applicable to the π-electron system of various heteroaromatic systems and to σ lone pair electrons (n) for nitrogen-containing molecules (see [3] for references). An extension of the PPP-method to organometallic molecules was suggested by Roos [4]. This method has been applied to Cu complexes [4–7] and has given very promising results. In the present work the scheme is extended to include iron complexes. The method has been thoroughly presented previously [4, 7] and will only be shortly outlined here:

1. The method is based on the Roothaan MO-SCF method for open shell systems [20].

2. The electrons have been divided into two groups, the core and the peel. The core group is not explicitly taken into account; it merely contributes a constant charge density, corresponding to a fixed electrostatic potential field. The Hamiltonian of the peel electrons can be written:

$$H = \sum_i H_{(i)}^{\text{core}} + \sum_{i<j} 1/r_{ij} \tag{1}$$

where $H_{(i)}^{\text{core}}$ is the sum of the kinetic and potential energy operator for electron i. The peel consists of the valence electrons of the metal atom, the ligand lone-pair electrons, and the π electrons of the ligands. The molecular orbitals are given as linear combinations of atomic orbitals, which are taken to be: 3*d*, 4*s* and 4*p* orbitals on the metal atom, σ lone-pair orbitals for the ligand atoms, and one π orbital for each of the atoms contributing π-electrons to the system.

3. The zero differential overlap (ZDO) approximation is applied to all two-electron integrals except for the one-center exchange integrals.

4. Only resonance integrals between neighbouring atoms are retained, in correspondance with the nature of the ZDO approximation.

5. The method is semi-empirical. The following integrals are determined from atomic or molecular ionization potentials and spectral data:

Resonance integrals, $\beta_{\mu\nu} = H_{\mu\nu}^{\text{core}}$ (μ and ν neighbours),

two-center coulomb integrals, $\gamma_{\mu\nu}$ (μ and ν neighbours),

one-center coulomb integrals, $J_{\mu\nu}$,

one-center exchange integrals, $K_{\mu\nu}$,

parts of the one-center core integrals, $\alpha_\mu = H_{\mu\mu}^{\text{core}}$.

α_μ is decomposed according to a technique due to Goeppert-Mayer and Sklar [22], and described further in next section.

6. Excited states are calculated by means of the method of superposition of configurations. All types of singly excited configuration are included.

4. Semiempirical Iron Parameters

The extended PPP-method can be formulated in terms of two types of integrals: one-electron integrals occurring in the core matrix H^{core}, and two-electron integrals of coulomb and exchange type. In a semiempirical theory these integrals should be expressible in terms of a limited set of semiempirical parameters. The idea is to determine as many as possible of these parameters from experimental data. A general scheme using experimental data has been developed for the evaluation of semiempirical parameters of carbon and hetero atoms (see [3] for further references). In the present work previously determined carbon and nitrogen parameters [1, 3] have been used.

Semiempirical parameters for the iron atom and for the iron ligand bond have been derived in the present work and will be discussed in detail. It should be stressed that the procedure to obtain these parameters necessarily must be more uncertain depending on the greater complexity, e.g. the metal atom contributes nine AO's to the basis set, and the lack of sufficient experimental information.

Two-Electron Integrals

1. One-center coulomb, $J_{\mu\nu}$, and exchange, $K_{\mu\nu}$, integrals are considered and expressed in terms of Slater-Condon parameters F_k and G_k [40, 41]. These parameters were determined from iron atomic spectra and atomic Hartree-Fock calculations (see Appendix 1). They are considered dependent on charge, q, or number of d-electrons, n_d. Values obtained are given in Table 1.

2. Of the two-center two-electron integrals only the coulomb integrals, $\gamma_{\mu\nu}$, are retained. They were calculated by means of an interpolation formula suggested by Roos [4, 21]:

$$\gamma_{\mu\nu}(R) = \tfrac{1}{2}(\gamma_{\mu\mu} + \gamma_{\nu\nu}) \cdot f(z) \tag{2}$$

where R is the distance between the orbitals,

$$z = \tfrac{1}{2}(\gamma_{\mu\mu} + \gamma_{\nu\nu}) R \tag{3a}$$

and

$$f(z) = 1/(z + e^{-z}) . \tag{3b}$$

Formula (2) is independent of the orientation of local coordinate axes.

Table 1. One-center semiempirical parameters (in kK) for Fe

SCP[a] \ q[b]	$q=0$	$q=+1$	$q=+2$
ε_s	−490.37	−560.95	−612.78
$F_0(ss)$	49.70	58.29	—
$F_0(sd)$	62.17	73.12	84.06
$G_2(sd)$	1.290	1.560	1.830
ε_p	−356.83	−449.38	−481.79
$F_0(pp)$	43.74	55.24	—
$F_2(pp)$	0.919	1.160	
$F_0(sp)$	46.72	56.77	—
$G_1(sp)$	10.023	12.573	—
$G_1(pd)$	0.324	0.478	0.632
$G_3(pd)$	0.0162	0.0239	0.0316
$F_0(pd)$	46.66	61.42	68.47
$F_2(pd)$	0.275	0.351	0.411

SCP \ n_d[c]	$n_d=8$	$n_d=7$	$n_d=6$	$n_d=5$
ε_d	−734.40	−767.93	−793.83	−808.48
$F_0(dd)$	95.89	105.54	115.19	124.84
$F_2(dd)$	1.075	1.246	1.418	1.589
$F_4(dd)$	0.096	0.105	0.114	0.123

[a] SCP stands for Slater-Condon parameter.
[b] q is the charge of the iron ion.
[c] n_d is the number of 3d electrons of the iron ion.

One-Electron Integrals

The one-electron operator H^{core} has the following form:

$$H^{\text{core}} = T + U^{\text{core}}(\text{Me}) + \sum_i U^{\text{core}}(L_i) \tag{4}$$

where T denotes the kinetic energy operator, $U^{\text{core}}(\text{Me})$ the potential field from the metal core and $U^{\text{core}}(L_i)$ the corresponding field from the ligand atom i.

1. The core integral α_μ, where μ is a metal atomic orbital, can be decomposed in the following way:

$$\alpha_\mu = \varepsilon_\mu - \sum_i \sum_{\nu(i)} n_{\nu(i)} \gamma_{\mu\nu(i)} + \Delta\alpha_\mu \tag{5}$$

where

$$\varepsilon_\mu = \langle \mu | T + U^{\text{core}}(\text{Me}) | \mu \rangle \tag{6}$$

and

$$\Delta\alpha_\mu = \Sigma \langle \mu | \mathrm{U}^0(L_i) | \mu \rangle . \tag{7}$$

This technique to rewrite α_μ is due to Goeppert-Mayer and Sklar [22]. ε_μ contains the interaction between a metal electron and the metal core. The matrix elements, ε_μ, were determined from atomic ionization potentials and atomic spectral data (see Appendix 1 and Table 1). In the second part of (5) $n_{\nu(i)}$ is the number of electrons

associated with the atomic orbital $v(i)$ at the ligand atom i. $\Delta\alpha_\mu$ represents the penetration between a metal orbital and a neutral atom and was roughly estimated as follows: The nitrogen atoms were treated as point dipoles (in the center of the nitrogen atom) with a dipole moment of 2.25 D corresponding to the dipole moment of pyridine [23] and with a direction opposite to the vector connecting the center of the nitrogen atom to the center of charge of the sp^2-hybridized lone pair of nitrogen. $\Delta\alpha_\mu$ was estimated as the interaction between these dipoles and an electronic charge situated at the center of charge of the orbital μ. This method gave a value of 0.367 a.u. for the bipy complex and a value of 0.359 a.u. for the GMI complex. In this context it should be noted that it would be desirable to consider the sum of the first and third terms of (5) as one parameter to be determined from experimental data; e.g., ionization potentials of a series of similar iron complexes, thus applying a method similar to the one used for π systems. Unfortunately the lack of experimental data confines us to use the present much cruder method.

The core integrals $\alpha_{v_C(\pi)}$, $\alpha_{v_N(\pi)}$, and $\alpha_{v_N(n)}$, where $v_C(\pi)$, $v_N(\pi)$ and $v_N(n)$ are ligand atomic orbitals, are also decomposed according to the Goeppert-Mayer and Sklar method:

$$\alpha_{v_C(\pi)} = W_{v_C(\pi)} - \sum_{v' \neq v_C(\pi)} n_{v'} \gamma_{v' v_C(\pi)} - \sum_{\mu} n_\mu \gamma_{\mu v_C(\pi)} + \langle v_C(\pi) | U^0(\mathrm{Me}) | v_C(\pi) \rangle ; \quad (8)$$

$$\alpha_{v_N(\pi)} = W_{v_N(\pi)} - 2J_{v_N(\pi) v_N(n)} + K_{v_N(\pi) v_N(n)} - \sum_{v' \neq \{v_N(\pi) \text{ and } v_N(n)} n_{v'} \gamma_{v' v_N(\pi)} - \sum_{\mu} n_\mu \gamma_{\mu v_N(\pi)} + \langle v_N(\pi) | U^0(\mathrm{Me}) | v_N(\pi) \rangle ; \quad (9)$$

$$\alpha_{v_N(n)} = W_{v_N(n)} - J_{v_N(\pi) v_N(n)} + \tfrac{1}{2} K_{v_N(\pi) v_N(n)} - \sum_{v' \neq \{v_N(\pi) \text{ and } v_N(n)} - \sum n_\mu \gamma_{\mu v_N(n)} + \langle v_N(n) | U^0(\mathrm{Me}) | v_N(n) \rangle ; \quad (10)$$

v' denotes a ligand atomic orbital and μ a metal atomic orbital. In the present work the terms expressing the ligand metal penetration, $\langle v | U^0(\mathrm{Me}) | v \rangle$, have been neglected as was also done in previous calculations on copper complexes. The parameters W_v are discussed in detail in previous papers [1, 3, 19].

2. The formula of Wolfsberg and Helmholtz [24] was used for the resonance integrals $\beta_{\mu v}$,

$$\beta_{\mu v} = -\frac{k_\mu}{2} \cdot S_{\mu v} (I_\mu + I_v) \quad (11)$$

where μ is a metal orbital (3*d*, 4*s*, or 4*p*) and v an orbital of the nitrogen atoms.

Here I_μ and I_v are valence state ionization potentials, $S_{\mu v}$ the overlap integral between μ and v, and k_μ constants to be determined from molecular spectral data[2]. The overlap integrals were calculated theoretically from atomic Hartree-Fock orbitals for iron [25, 26] and nitrogen [26]. In line with previous studies on copper complexes, the preliminary intention was to investigate whether three different values, k_{3d}, k_{4s}, and k_{4p}, could be determined from the electronic spectral data of the bipyridyl and GMI complexes of iron(II). The initial values for these parameters were taken from previous studies of copper complexes [4, 5]. The calculated

[2] The assumed occupation numbers in determining the metal I_μ values are $3d^6 4s 4p$ for 4*p* and $3d^6 4s^2$ for 4*s* and 3*d*.

spectra were found to be predominantly determined by the value of k_{3d}. A satisfactory agreement between theory and experiment was obtaines for $k_{3d} = 3.26$ and $k_{4s} = k_{4p} = 1.0$. It should be noted, however, that the calculated spectra are insensitive to moderate changes in k_{4s} and k_{4p}.

5. Details of the Calculation

As far as we know there are no X-ray diffraction data for the iron(II) complexes with *tris*-(2,2′-bipy) and *tris*-(GMI). From an analysis of measured NMR spectra of $[Fe(II)\text{-}(dipy)_3]Cl_2$ Castellano, Günther and Ebersole [27] concluded that the *cis*-planar conformation of the bipyridyl groups was in line with the measured values of the chemical shifts. They also derived a metal-nitrogen distance of 2 Å. For a similar complex, *tris-o*-phenanthroline iron(II), Templeton, Zalkin and Ueki [28] obtained an average iron-nitrogen distance of 1.97 Å. In the present calculations of the two diamagnetic complexes $[Fe(II)\text{-}(bipy)_3]^{++}$ and $[Fe(II)\text{-}(GMI)_3]^{++}$ the Fe–N distance is assumed to be 2.0 Å. This is also in accord with recent X-ray data on a high-spin and a low-spin form of $Fe(dipy)_2(NCS)_2$ by König and Watson [29]. They obtained an average Fe–N distance of about 2.02 Å for the low spin (singlet) form. Both complexes are assumed to have D_3 symmetry. The dipyridyl ligands are assumed to have *cis*-planar structure with the same interatomic distances as found from electron diffraction measurements [30]. This structure was also used in a previous MO calculation [31] on the planar *cis*- and *trans*-forms of bipyridyl.

There are no experimental structural data of GMI. A first separate MO calculation was performed for GMI with the same reasonable assumption of geometry as was made by Ito *et al.* [14] in their theoretical investigation of GMI and the *tris*-(GMI) iron(II) complex. New bond distances were obtained from the calculated bond orders, $p_{\mu\nu}$, by means of the relations [1, 19]

$$R_{\mu\nu}(C, C) = 1.517 - 0.18\, p_{\mu\nu}\,, \tag{12}$$

$$R_{\mu\nu}(C, N) = 1.458 - 0.18\, p_{\mu\nu}\,. \tag{13}$$

The calculation on GMI was repeated with the obtained bond distances and with angles for GMI such that in the iron complex the N–Fe–N angle would be 90° for the Fe–N distance equal to 2.0 Å. The structures of GMI and dipy are shown in Fig. 1 and the interatomic distances used in the calculations are given in Table 2.

Table 2. Bond distances (in Å) for GMI and bipyridyl chosen for the calculations. The numbering of the atoms are given in Fig. 1 and in text (Section 5)

GMI		Bipyridyl	
Bond	Bond length	Bond	Bond length
4—1	1.4600	4— 1	1.4700
7—1	1.2878	7— 1; 13— 7	1.3394
Fe–N	2.0000	19—13; 31— 1	1.3958
		25—19; 31—25	1.3936
		Fe–N	2.0000

Both in the calculation of GMI and $(Fe(II)\text{–}(GMI)_3]^{++}$ the influence of the CH_3 groups was neglected.

The propellershaped structure of the complexes is visualized in Fig. 2, where the three ligands are denoted A, B and C. The calculations were performed for the right-handed optical isomers [32].

In the following, x, y, z denotes the coordinate system adopted to D_3 symmetry. The z-axis is taken as the threefold symmetry axis, and the x- and y-axes are taken to form a right-handed system with the positive x-axis passing through the twofold axis of ligand A (cf. Fig. 2).

$$\begin{aligned} \hat{x} &= \frac{1}{\sqrt{2}}(\hat{\xi} - \hat{\eta}) \\ \hat{y} &= \frac{1}{\sqrt{2}}(\hat{\xi} + \hat{\eta} - 2\hat{\zeta}) \\ \hat{z} &= \frac{1}{\sqrt{2}}(\hat{\xi} + \hat{\eta} + \hat{\zeta}) . \end{aligned} \tag{14}$$

This same choice of axes was also made by Day and Sanders [11].

The numbering of the atomic orbitals in ligand A is given in Fig. 1. If i numbers an AO on ligand A, $(i+1)$ will number the corresponding AO on ligand B, and $(i+2)$ the corresponding AO on ligand C.

The atomic orbitals that constitute the basis for the calculations are 27 for the GMI complex and 51 for the dipy complex: the 3*d*, 4*s* and 4*p* orbitals of the iron ion, one sp^2 hybridized lone pair orbital (n) from each nitrogen, and one π orbital from each of the carbon and nitrogen atoms of the ligands. For the GMI-complex the atomic orbitals with numbers from 1–12 refer to ligand π orbitals, while for the dipy complex, 1–36 refer to π orbitals. The number of electrons taken into account is 30 in the GMI complex and 54 in the dipy complex; in each complex, 6 electrons come from the iron ion and the rest from the ligands.

The self-consistent field molecular orbitals were evaluated by means of a computer program, SCF–OPSZDO, written by B. Roos and M. Sundbom. This program also calculates the energy levels of excited states by mixing configurations from single excitations. All computations were made on an IBM 360/75 computer. The program and the computer limit the number of configurations for each symmetry to 140. Thus for the bipy complex not all of the single excitations could be considered. The CI treatment was restricted for each symmetry to 140 configurations.

The values of the one-center semiempirical parameters of iron depend on the electronic population of the iron ion (see appendix). A reasonable guess of the electronic population was made from Mössbauer isomer shift data, according to a method presented in a previous publication [33]. The initial effective configuration of the iron ion was thus guessed to be $(3d)^{5.75}\,(4s)^{0.5}\,(4p)^{0.5}$. The values of the one-center parameters for this configuration were obtained by interpolation in Table 1 and were used in the preliminary calculations to obtain reasonable values of the parameters k_μ, which occur in the expressions for the resonance integrals (cf. Section 3). When reasonable values for k_μ had been obtained, new one-center iron

parameters were determined from the calculated effective configuration. The whole calculation was repeated with these new parameters. This procedure was repeated until self-consistency was achieved. In view of the simplified electron configuration dependence of the one center iron parameters (see appendix) the calculation was repeated only if the calculated values of n_{3d} and q deviated from the input values by more than ± 0.1. This selfconsistency in charge procedure was then repeated for each set of trial k_μ values.

6. Molecular Orbitals and Ground State Properties

The SCF molecular orbitals and eigenvalues of $[Fe(II)\text{–}(GMI)_3]^{++}$ are presented in Tables 3 and 4. The orbital pattern is similar for both compounds.

$[Fe(II)\text{–}(GMI)_3]^{++}$

From Table 4 where the total electron population of the atomic orbitals is given, the configuration of the Fe ion is found to be $(3d)^{5.46}\,(4s)^{0.42}\,(4p)^{0.42}$ with a net charge of $+1.70$ on iron. The Table 4 contains a comparison with the elec-

Table 3. Molecular orbitals of $[Fe(II)\text{–}(GMI)_3]^{++}$. Orbital energies ε_i in a.u. The electronic population. The numbering system as in Fig. 1

MO[a]			The electron population[b,c]								
No.	Sym-metry	ε_i	C_1	N_7	n_7	z^2	$xy+(x^2-y^2)$	$xz+yz$	s	$x+y$	z
1	$1a_1$	−1.0887	0.000	0.000	0.131	0.004	0	0	0.209	0	0
2;3	$1e$	−1.0706	0.000	0.000	0.260	0	0.147	0.292	0	0.001	0
4	$1a_2$	−0.9736	0.001	0.003	0.150	0	0	0	0	0	0.079
5;6	$2e$	−0.9642	0.004	0.013	0.290	0	0.019	0.013	0	0.126	0
7;8	$3e$	−0.8801	0.094	0.179	0.023	0	0.155	0.062	0	0.001	0
9	$2a_1$	−0.8597	0.014	0.090	0.000	0.372	0	0	0.002	0	0
10	$2a_2$	−0.8542	0.075	0.087	0.004	0	0	0	0	0	0.002
11;12	$4e$	−0.8027	0.072	0.249	0.000	0	0.050	0.019	0	0.001	0
13	$3a_1$	−0.6774	0.027	0.039	0.000	0.598	0	0	0.002	0	0
14;15	$5e$	−0.6567	0.141	0.024	0.001	0	0.754	0.245	0	0.000	0
16	$3a_2$	−0.4066	0.091	0.073	0.001	0	0	0	0	0	0.011
17;18	$6e$	−0.3407	0.100	0.121	0.001	0	0.507	0.120	0	0.038	0
19;20	$7e$	−0.2539	0.254	0.070	0.000	0	0.052	0.003	0	0.001	0
21	$4a_1$	−0.2490	0.126	0.037	0.000	0.025	0	0	0.000	0	0
22;23	$8e$	−0.1818	0.001	0.001	0.072	0	0.314	1.246	0	0.000	0
24	$5a_1$	−0.0964	0.000	0.000	0.035	0.001	0	0	0.788	0	0
25;26	$9e$	0.0107	0.001	0.008	0.018	0	0.002	0.000	0	1.831	0
27	$4a_2$	0.0252	0.000	0.003	0.012	0	0	0	0	0	0.908

[a] The 15 lowest orbitals are doubly occupied.

[b] Formal population of the virtual orbitals.
N_7 and C_1 denotes π orbitals on nitrogen and carbon. n_7 denotes a nitrogen σ lone pair orbital. z^2 stands for $3d_{z^2}$, s for $4s$ and x for $4p_x$ on iron.

[c] For orbitals of e symmetry the sum of population for e_x and e_y is given.

Table 4. The electronic population of the atomic orbitals in $[Fe(II)\text{–}(GMI)_3]^{++}$, GMI *(cis)* and GMI *(trans)*

AO	$[Fe(II)\text{–}(GMI)_3]^{++}$	GMI *(cis)*	GMI *(trans)*
GMI:			
C	0.856	0.981	0.979
N	1.372	1.019	1.021
n	1.721	2.000	2.000
Fe:			
z^2	1.947	$n_{3d} = 5.457$	
$x^2 - y^2; xy$	1.124		
$yz; xz$	0.631		
s	0.424	$n_{4s} = 0.424$	$q = 1.701$
$x; y$	0.128	$n_{4p} = 0.418$	
z	0.162		

tronic population in GMI. Further, this table shows that there is a synergic interaction between metal-ligand σ- and π-bonding, resulting in a net transfer of electrons from the ligand σ system to mainly the 4*s*, 4*p* and 3*d* orbitals of Fe and in a backdonation from the 3*d* orbitals to the ligand π system.

The value of the electronic density at the iron nucleus, $|\psi(0)|^2$, deduced from the calculated effective configuration of valence electrons by a recently published method [33], is in good agreement with the value obtained from the measured Mössbauer isomer shift (Table 5).

As shown in Table 3 the molecular orbital $1a_1$ is mainly a ligand nitrogen lone pair orbital, stabilized by bonding to Fe 4*s* (21%). $2a_1$ is a bonding and $3a_1$ an antibonding metal-ligand (π) orbital with 37% and 60% d_{z^2}-character respectively. The orbital $1a_2$ is a ligand n orbital weakly stabilized by $4p_z$ (8%), while $2a_2$ can be considered as a pure ligand π orbital. As shown in Table 3 $1e$ is mainly a ligand n-orbital (22% *d*-character), $2e$ is a ligand n orbital, while $3e$ and $4e$ are ligand π orbitals. $5e$ has 50% metallic 3*d* and 50% ligand π character.

The results of the present MO study show that only one orbital ($3a_1$) is mainly (60%) metallic, indicating the difficulty in discussing this compound from the crystal field point of view. In many previous discussions the splitting of the octahedral levels have been considered small and generally neglected. This assumption is not justified by the present results.

$[Fe(II)\text{–}(bipy)_3]^{++}$

The orbital pattern resembles that of the GMI complex.

The configuration of the Fe ion is found to be $(3d)^{5.47}\,(4s)^{0.42}\,(4p)^{0.42}$ with a net charge of 1.69 on iron. As shown in Table 5, the calculated effective electronic configuration yields a value of the electronic density at the nucleus in accord with the value obtained from the observed Mössbauer isomer shift. The good agreement

Table 5. The electron density at the Fe nucleus, $|\psi(0)|^2$, for $[Fe(II)\text{–}(GMI)_3]^{++}$ and $[Fe(II)\text{–}(bipy)_3]^{++}$. Calculated values compared with values derived from experimental Mössbauer isomer shifts, δ [33]

	Calculation	Observations					
		Epstein [34]				Present work	
	$\|\psi(0)\|^2$	δ[a] (mm/s) at 300° K	$\|\psi(0)\|^2$	δ[a] (mm/s) at 80° K	$\|\psi(0)\|^2$	δ[a] (mm/s) at 300° K	$\|\psi(0)\|^2$
$[Fe(II)\text{–}(GMI)_3]^{++}$	11907.75	0.414 ±0.010[b]	11907.53 ±0.04	0.515 ±0.013[b]	11907.17 ±0.04	0.27 ±0.01[c]	11908.04 ±0.04
$[Fe(II)\text{–}(bipy)_3]^{++}$	11907.66	0.367 ±0.008[b]	11907.70 ±0.03	0.403 ±0.005[b]	11907.57 ±0.02	0.41 ±0.01[d]	11907.55 ±0.04

[a] Relative stainless steel (SS). (Add 0.161 mm/s to convert to sodium nitroprusside as references substance.)
[b] The perchlorate salts.
[c] $Fe\text{–}(GMI)_3I_2$.
[d] $Fe\text{–}(bipy)_3 \cdot SO_4 \cdot 5H_2O$.

between theoretical and experimental values indicates that the present MO method can be used with some confidence for the determination of the electronic distribution in transition metal complexes.

The orbital pattern shows that O_h symmetry will not be adequate for the assignment of electronic transitions. Distortions due to the actual D_3 symmetry are considerable and cannot be neglected. Furthermore no orbital can be considered as purely metallic, thus indicating that crystal field theory cannot be used to give a realistic picture of the electronic energy levels.

7. Excited States

The present CI treatment allows a quantitative description of the excited electronic energy levels. The calculations show that it is possible to classify only a few of the excited states as pure $d-d$, $\pi-\pi^*(L)$, or CT transitions. This was also found in previous calculations on organic copper complexes [4–7]. The results are presented in Tables 6–12. For comparison the spectra of planar *cis*- and *trans*-forms of GMI and bipyridyl have also been calculated (for bipyridyl, see Ref. [31]). The values obtained are given together with experimental data in Table 12.

$[Fe(II)\text{–}(GMI)_3]^{++}$

Most transitions can be classified as partly CT and partly L. The observed intense visible band at 18 kK is assigned to the $3\,^1E$ state (calc. 19.9 kK), which is mainly a combination of the configurations $(5e \rightarrow 6e)$ and $(5e \rightarrow 3a_2)$ (Table 8). They both have some $d \rightarrow \pi^*$ character. The amount of electron transfer is 0.25, as shown in Table 9, where the electronic populations for some of the excited states are given.

Table 6. Electronic singlet transitions in $[Fe(II)\text{–}(GMI)_3]^{++}$. Transition frequencies in kK

Type[a]	Symmetry	Calculated		Observed				
				Ito *et al.* [14][b]		Present investigation		
		ν	f	ν_{max}	$\log\varepsilon_{max}$	ν_{max}	Range	$\log\varepsilon_{max}$
$CT+L$	$1\,^1A_2$	14.1	0.0003					
$\underline{CT}+d-d$	$1\,^1E$	14.3	0.00003					
CT	$2\,^1A_2$	15.2	0.004					
$CT+L$	$2\,^1E$	15.3	0.004					
$CT+L$	$3\,^1E$	19.9	0.38	18.5	3.9	18.0		3.94
$d-d$	$4\,^1E$	21.8	0.0008	19.4[s]	3.8	19.8[s]	17–22	3.79
$CT+d-d$	$5\,^1E$	30.9	0.03	29.1	2.3		28.5–29.4	very weak
$CT+d-d$	$3\,^1A_2$	31.0	0.0004					
$CT+d-d$	$1\,^1A_1$	32.3	0					
$CT+L$	$2\,^1A_1$	37.3	0					
$CT+L$	$4\,^1A_2$	48.4	0.17	45.0[s]	4.0	44.3	42–47.5	4.55
$CT+L$	$6\,^1E$	48.5	0.01					
$CT+L$	$7\,^1E$	50.4	0.05					
$CT+\underline{L}$	$8\,^1E$	50.6	0.21					
$CT+L$	$3\,^1A_1$	50.9	0					
$\underline{CT}+L$	$9\,^1E$	51.5	0.16					
$CT+L$	$4\,^1A_1$	55.1	0					
L	$10\,^1E$	59.9	0.03					
$CT+L$	$5\,^1A_2$	60.2	0.40	54.7	4.6	54	47.5→54	4.8

[a] CT = charge transfer; L = intraligand $\pi-\pi^*$.

[b] *tris*(glyoxal-*bis*-N-methylimine) iron(II) tetrafluoroborate in an aqueous solution. The values are estimated from Fig. 1 in [14b].

Table 7. The lower electronic singlet and triplet transitions in $[Fe(II)\text{–}(GMI)_3]^{++}$. Calculated values and the estimated range in which to search for the transition

Type	Symmetry	Calculated		Estimated range,
		ν (kK)	f	ν (kK) (cf. text)
$CT+L$	$1\,^3A_1$	4.6	0	3—10
$CT+L$	$1\,^3E$	5.7	0	4—11
$CT+d-d$	$2\,^3E$	7.9	0	6—13
$CT+L$	$1\,^3A_2$	8.6	0	7—12
$CT+L$	$3\,^3E$	12.7	0	17—18
$d-d$	$4\,^3E$	13.8	0	12—19
$CT+L$	$1\,^1A_2$	14.1	0.0003	10—12
$CT+L$	$2\,^3A_2$	14.1	0	12—13
$CT+d-d$	$1\,^1E$	14.3	0.00003	10—12
CT	$2\,^1A_2$	15.2	0.004	11—13
$CT+L$	$2\,^1E$	15.3	0.004	11—13
$CT+L$	$3\,^1E$	19.9	0.38	18.0[a]
$d-d$	$4\,^1E$	21.8	0.008	19.8[a]
$CT+d-d$	$3\,^3A_2$	24.4	0	22—29[b]
$CT+d-d$	$5\,^3E$	24.5	0	22—29[b]
$CT+d-d$	$2\,^3A_1$	24.7	0	22—29[b]
$CT+d-d$	$5\,^1E$	30.9	0.03	~29[a]

[a] Observed. See Table 6.

[b] Ito *et al.* [14] observed a shoulder band near 25 kK, that may be assigned to one or all of the three triplets: $3\,^3A_2$, $5\,^3E$ and $2\,^3A_1$.

Table 8. The lower excited states of $[Fe(II)\text{–}(GMI)_3]^{++}$. Configuration mixing[a]

Symmetry	Wave function
$1\,^3A_1$	$0.96\,(5e \rightarrow 6e)^T$
$1\,^3E$	$-0.62\,(5e \rightarrow 6e)^T + 0.25\,(3a_1 \rightarrow 6e)^T + 0.72\,(5e \rightarrow 3a_2)^T$
$2\,^3E$	$0.45\,(5e \rightarrow 6e)^T + 0.83\,(3a_1 \rightarrow 6e)^T$
$1\,^3A_2$	$0.52\,(5e \rightarrow 6e)^T + 0.81\,(3a_1 \rightarrow 3a_2)^T$
$3\,^3E$	$0.59\,(5e \rightarrow 6e)^T - 0.38\,(3a_1 \rightarrow 6e)^T + 0.66\,(5e \rightarrow 3a_2)^T$
$4\,^3E$	$0.92\,(3a_1 \rightarrow 8e)^T + 0.39\,(2a_1 \rightarrow 8e)^T$
$1\,^1A_2$	$0.98\,(5e \rightarrow 6e)^S$
$2\,^3A_2$	$0.82\,(5e \rightarrow 6e)^T - 0.51\,(3a_1 \rightarrow 3a_2)^T$
$1\,^1E$	$0.28\,(5e \rightarrow 6e)^S + 0.91\,(3a_1 \rightarrow 6e)^S - 0.23\,(2a_1 \rightarrow 6e)^S$
$2\,^1A_2$	$0.99\,(3a_1 \rightarrow 3a_2)^S$
$2\,^1E$	$0.66\,(5e \rightarrow 6e)^S - 0.25\,(3a_1 \rightarrow 6e)^S + 0.66\,(5e \rightarrow 3a_2)^S$
$3\,^1E$	$-0.61\,(5e \rightarrow 6e)^S + 0.72\,(5e \rightarrow 3a_2)^S$
$4\,^1E$	$0.92\,(3a_1 \rightarrow 8e)^S - 0.36\,(2a_1 \rightarrow 8e)^S$
$3\,^3A_2$	$0.95\,(5e \rightarrow 8e)^T$
$5\,^3E$	$0.96\,(5e \rightarrow 8e)^T$
$2\,^3A_1$	$0.96\,(5e \rightarrow 8e)^T$
$5\,^1E$	$0.95\,(5e \rightarrow 8e)^S$
$3\,^1A_2$	$0.96\,(5e \rightarrow 8e)^S$
$1\,^1A_1$	$0.96\,(5e \rightarrow 8e)^S$
$2\,^1A_1$	$0.83\,(5e \rightarrow 6e)^S - 0.42\,(3a_1 \rightarrow 4a_1)$
$4\,^1A_2$	$0.96\,(5e \rightarrow 7e)^S$
$6\,^1E$	$0.79\,(5e \rightarrow 7e)^S + 0.56\,(5e \rightarrow 4a_1)$
$7\,^1E$	$0.85\,(4e \rightarrow 3a_2)^S + 0.39\,(3a_1 \rightarrow 7e)$
$8\,^1E$	$-0.50\,(5e \rightarrow 7e)^S + 0.80\,(5e \rightarrow 4a_1) + 0.20\,(4e \rightarrow 3a_2)$
$3\,^1A_1$	$0.85\,(5e \rightarrow 7e)^S - 0.52\,(3a_1 \rightarrow 4a_1)$
$9\,^1E$	$0.95\,(3a_1 \rightarrow 7e)^S - 0.43\,(4e \rightarrow 3a_2)$
$4\,^1A_1$	$0.52\,(4e \rightarrow 6e)^S + 0.34\,(5e \rightarrow 7e) + 0.28\,(5e \rightarrow 6e)$
$10\,^1E$	$0.96\,(4e \rightarrow 6e)^S$

[a] T stands for triplet, and S for singlet.

Table 9. Populations for some excited states in $[Fe(II)\text{–}(GMI)_3]^{++}$

State	$3d_{z^2}$	$3d_{x^2-y^2}+3d_{xy}$	$3d_{xz}+3d_{yz}$	$4s$	$4p_x+4p_y$	$4p_z$	C(π)	N(π)	N(n)
Ground[a]	1.947	2.248	1.262	0.424	0.256	0.162	5.139	8.229	10.328
$1\,^3A_1$[b]	0.000	−0.172	−0.081	0.000	0.018	0.000	−0.064	0.302	− 0.002
$2\,^1E$[b]	−0.057	−0.232	−0.108	0.000	0.012	0.006	0.074	0.301	0.004
$3\,^1E$[b]	−0.043	−0.242	−0.024	0.000	0.010	0.006	0.036	0.330	0.000
$4\,^1E$[b]	−0.881	0.222	0.553	−0.002	0.001	0.000	−0.074	−0.035	0.217
$5\,^1E$[b]	−0.001	−0.368	0.518	0.000	0.000	0.000	−0.270	−0.075	0.196
$4\,^1A_2$[b]	−0.003	−0.379	−0.123	0.000	0.000	0.000	0.389	0.122	− 0.007
$7\,^1E$[b]	−0.107	−0.042	−0.011	0.001	0.000	0.012	0.380	−0.231	− 0.003
$8\,^1E$[b]	−0.004	−0.363	−0.117	0.000	0.000	0.001	0.410	0.079	− 0.006
$9\,^1E$[b]	−0.526	−0.017	−0.006	−0.001	0.001	0.003	0.581	−0.035	− 0.001
$5\,^1A_2$[b]	−0.207	0.039	0.015	0.005	0.004	0.014	0.362	−0.205	− 0.026

[a] Populations.
[b] Change from the ground state population.

Table 10. Electronic singlet transitions in $[Fe(II)–(bipy)_3]^{++}$. Transition frequencies in kK

Type	Symmetry	Calculated		Observed				
				Present investigation[a]			Hanazaki and Nagakura[b] [15]	
		ν	f	ν_{max}	range	$\log\varepsilon_{max}$	ν	$\log\varepsilon$
$CT+L$	$1\,^1A_2$	11.2	0.004					
$CT+L$	$1\,^1E$	13.1	0.03					
CT	$2\,^1E$	15.9	0.35	19.2	18—23	3.86	19.5	3.93
$CT+d-d$	$3\,^1E$	17.3	0.003	20.5[s]		3.80	20.4[s]	3.87
CT	$2\,^1A_2$	22.4	0.003	24.1	23—24.5	3.18	24.2[s]	3.38
$CT+L$	$1\,^1A_1$	25.6	F	25.5[s]	24.5—31	3.45	25.6[s]	3.54
$CT+L$	$4\,^1E$	27.7	0.04					
$CT+L$	$3\,^1A_2$	28.1	0.29	28.6		3.75	28.74	3.81
$CT+L$	$5\,^1E$	29.0	0.20	29.8[s]		3.67		
$CT+L$	$2\,^1A_1$	31.5	F					
$CT+L$	$6\,^1E$	31.8	0.00004					
$d-d$	$7\,^1E$	32.8	0.0005					
$CT+L+d-d$	$8\,^1E$	33.6	0.004					
$CT+L+d-d$	$4\,^1A_2$	33.8	0.02					
$CT+L$	$9\,^1E$	33.9	0.10					
$CT+L$	$5\,^1A_2$	34.6	0.18					
$CT+L$	$10\,^1E$	36.7	0.15					
CT	$11\,^1E$	37.5	0.39	33.4	32—36	4.77	33.56	4.81
$CT+L$	$6\,^1A_2$	37.9	0.91	34.5[s]		4.72	34.5[s]	4.74
$CT+L$	$12\,^1E$	40.4	0.02					
$CT+L$	$7\,^1A_2$	40.7	0.31	38.6[s]	36—43	4.22	38.8[s]	4.26
$CT+L$	$13\,^1E$	42.2	0.13					
$CT+L$	$14\,^1E$	44.4	0.07					
$CT+L$	$8\,^1A_2$	44.7	0.95	40.5		4.41	40.49	4.44
$CT+L$	$15\,^1E$	44.9	0.29	42.0[s]		4.36	41.5[s]	4.38

The calculations give four singlets with energies lower than $3\,^1E$ and with low intensities.

A shoulder (19.8 kK) is observed on the high energy side of the 18 kK band and is probably due to the vibrational structure. A weak electronic transition, $4\,^1E$, is predicted to be found in that region. According to the form of the orbitals and the population analysis, the transition to $4\,^1E$ is a $d-d$ transition.

The three singlets $5\,^1E$ (30.9 kK), $3\,^1A_2$ (31.0 kK) and $1\,^1A_1$ (32.3 kK) all have $(5e\rightarrow 8e)$ as the main configuration, indicating that each of them can be classified as partly $d\rightarrow d$ and partly CT $(\pi\rightarrow d+d\rightarrow n)$ in character, as also shown in Table 9. The calculated weak transitions to $5\,^1E$ and $3\,^1A_2$ probably correspond to the observed weak band at 29 kK. Transitions to $^1A_1$ states are symmetry forbidden. Ito *et al.* [14] did not obtain any transition in this region, probably because $(d-d)$ transitions were not considered in their method.

Table 10 (continued)

Type	Symmetry	Calculated		Observed				
				Present investigation[a]			Hanazaki and Nagakura[b] [15]	
		ν	f	ν_{max}	range	$\log\varepsilon_{max}$	ν	$\log\varepsilon$
L	$16\,^1E$	47.6	0.07					
L	$17\,^1E$	47.7	0.01					
L	$9\,^1A_2$	47.7	0.10					
CT + L	$18\,^1E$	48.1	0.05					
CT + L	$10\,^1A_2$	48.8	0.11					
L	$19\,^1E$	50.1	0.009					
L	$20\,^1E$	50.7	0.03					
L	$11\,^1A_2$	52.1	0.005					
L	$21\,^1E$	52.7	0.31					
CT + L	$22\,^1E$	53.9	0.07					
L	$23\,^1E$	54.1	0.21					
L	$12\,^1A_2$	54.3	1.43	48.3[s]	43.5→	4.84	48[s]	4.70
L	$24\,^1E$	55.8	0.83					
L	$25\,^1E$	56.5	0.34					
L	$13\,^1A_2$	56.8	0.38					
L	$26\,^1E$	57.1	0.12					
L	$27\,^1E$	58.0	0.08					

[a] $[Fe(bipy)_3] \cdot SO_4 \cdot 5H_2O$ in methanol.
[b] $[Fe(bipy)_3] \cdot Cl_2 \cdot 7H_2O$ in aqueous solution.
[c] ^1E transitions are polarized perpendicular ($\perp$) to the C_3 axis.
$^1A_2$ transitions are polarized parallel ($\parallel$) with the C_3 axis.
$^1A_1$ transitions are symmetry forbidden.
[s] shoulder.

The $4\,^1A_2$ (48.4 kK) state is a combined CT ($d \rightarrow \pi^*$) and $L(\pi \rightarrow \pi^*)$ state (Table 9) and may be referred to the observed strong band at 44.3 kK.

Observations indicate a strong UV band at around 54 kK, also observed by Ito *et al.* [14]. It may be assigned to the $5\,^1A_2$ state that, according to the population analysis, can be classified as partly CT ($d \rightarrow \pi^*$) and partly $L(\pi \rightarrow \pi^*)$.

In Table 7 the lower calculated triplet and singlet transitions are given together with an estimated range in which to search for the transition. Calculated singlets with fairly safe assignments to observed transitions have been found to be around 2–4 kK too high in energy. The singlet-triplet gap will come out too large from the calculations, by 2–7 kK in the present method [3]. In the region 10–13 kK we predict two singlet transitions polarized parallel to the threefold z-axis, $1\,^1A_2$ and $2\,^1A_2$, and two singlets polarized perpendicular to the threefold z-axis, $1\,^1E$ and $2\,^1E$. The calculations further predict four low-lying triplets with some CT character, $1\,^3A_1$, $1\,^3E$, $2\,^3E$ and $1\,^3A_2$.

Table 11. The lower electronic singlet and triplet transitions in $[Fe(II)–(bipy)_3]^{++}$. Calculated values and the estimated range in which to search for the transition. Transition frequencies in kK

Type	Symmetry	Calculated		Estimated range, ν (cf. text)	Observed Present investigation[c]	
		ν	f		ν_{max}	$\log\varepsilon_{max}$
$CT+L$	$1\,^3A_1$	3.3		5—13[a]		
$CT+L$	$1\,^3E$	6.0		8—16[a]	8.85[d]	0.7
$CT+L$	$1\,^3A_2$	10.4		10—14[b]		
$CT+L$	$1\,^1A_2$	11.2	0.004	11—14[b]		
CT	$2\,^3E$	11.3		16—19[b]	11.8[d]	0.9
$CT+L$	$1\,^1E$	13.1	0.03	13—16[b]		
CT	$3\,^3E$	13.5		15—20[b]		
CT	$2\,^1E$	15.9	0.35	→	19.2	3.86
$CT+d-d$	$3\,^1E$	17.3	0.003	→	20.5[s]	3.80
$CT+L$	$2\,^3A_2$	18.7		22—24		
$CT+L$	$4\,^3E$	20.5		22—28		
$CT+L$	$3\,^3A_2$	21.8		23—28		
CT	$2\,^1A_2$	22.4	0.003	→	24.1[s]	3.18

[a] König and Schläfer [39] assigned a sharp peak at 8.98 kK to a triplet. This peak was later considered by Palmer and Piper [38] as the second overtone of the C–H stretching vibration.

[b] Palmer and Piper [38] observed a weak band located at 11.5 kK and assigned it as a spinforbidden transition ($3T_1 \leftarrow {}^1A_1$).

[c] $[Fe(bipy)_3]SO_4 \cdot 5H_2O$ in methanol (10^{-4} M).

[d] $[Fe(bipy)_3]SO_4 \cdot 5H_2O$ in aquaeus solution (0.3 M).

Table 12. Electronic singlet transition in *cis*- and *trans*-forms of bipyridyl. Transition frequencies in kK

Calculated						Observed [31] (cyclohexane)	
cis-			*trans*-				
Symmetry[a]	ν	f	Symmetry[a]	ν	f	ν_{max}	$\varepsilon_{max} \cdot 10^{-4}$
$^1B_1(n-\pi^*)$	36.0		$^1A_u(n-\pi^*)$	36.5			
$^1A_1$	39.0	0.02	^1B_u	38.8	0.08	35.5	1.50
$^1B_2$	39.3	0.05	^1A_g	39.4	0		
$^1B_2$	43.5	0.92	^1B_u	43.7	0.99	42.2	1.20
$^1B_1(n-\pi^*)$	47.5		$^1A_u(n-\pi^*)$	48.1			
$^1A_1$	51.8	0.17	^1A_g	50.4	0		
$^1B_2$	51.9	0.57	^1B_u	54.1	1.27	52.4	4.0
$^1B_2$	55.8	0.56	^1A_g	54.5	0		
$^1A_1$	57.3	0.42	^1A_g	57.4	0		
$^1A_1$	57.5	0.79	^1B_u	57.8	1.18		

[a] All transitions are $\pi - \pi^*$ unless otherwise indicated.

$[Fe(II)–(bipy)_3]^{++}$

The electronic spectra of this complex have been thoroughly investigated experimentally. A review of observed data can be found in three recent articles by König [35], Krumholz [36] and by Bryant, Fergusson and Powell [37]. Characteristic for the observed spectra are two intense bands in the visible at about 19 and 28 kK, and two strong bands in the ultraviolet at about 33 and

40 kK. In the following, these four bands and the region above 40 kK and below 20 kK will be discussed in more detail.

The Region Around 19 kK. The intense visible band at around 19 kK has been characterized as a CT band. Its intensity and its structure in crystal spectra [38] excludes a transition of $d-d$ type. It cannot be a perturbed ligand transition as no band is found for the ligand bipyridyl in that region (cf. Table 12).

The present calculations give only one strong band in this region, $2\,^1E$ (15.9 kK, Table 10), which is a CT ($d\rightarrow\pi^*$) transition, in accord with previous assignments.

The observed shoulder towards higher energy (20.4 kK) has been ascribed to a vibrational structure of the 19 kK band [32, 38]. The calculated $3\,^1E-2\,^1E$ separation (1.4 kK) indicates that the $d-\pi^*$ transition to $3\,^1E$ is to be found in that region. But as $3\,^1E$ is predicted to be much weaker than $2\,^1E$ (the calculated oscillator strength of $2\,^1E$ is 0.35 while it is only 0.003 for $3\,^1E$) it is probably hidden in the absorption spectra.

In between the two strong visible bands we have observed a weak band at 24.1 kK for $[Fe(bipy)_3]\cdot SO_4\cdot 5H_2O$ in methanol. Hanazaki and Nagakura [15] report a shoulder at 24.2 kK for $[Fe(bipy)_3]\cdot Cl_2\cdot 7H_2O$ in aqueous solution. This band may be assigned to the calculated weak $2\,^1A_2$ transition (22.4 kK, $f=0.003$) of $d\rightarrow\pi^*$ type. For a definite assignment to be made, a more careful analysis of polarization data in the narrow region (23–24.5 kK) remains to be done.

The Region Around 28 kK. Like Hanazaki and Nagakura [15] we assign the observed 28.6 kK band to three probably operlapping transitions, $4\,^1E$ (27.7 kK), $3\,^1A_2$ (28.1 kK) and $5\,^1E$ (29.0 kK) with f-values: 0.04, 0.29 and 0.20 respectively. They can all be classified as partly CT ($d\rightarrow\pi^*$) and partly $L(\pi\rightarrow\pi^*)$. As mentioned previously, in the GMI complex the transitions in this region have very low calculated f-values (0.03 and 0.0004) in accord with experimental findings. The difference of intensity for this band in the GMI and the bipyridyl complexes mirrors the fact that the bands are of different character in the two compounds.

The observed shoulder at 25.5 kK is most probably attributed to one of these three transitions, but it is interesting to note that the calculations also give an electronically forbidden transition in that region, to $1\,^1A_1$ (25.6 kK) characterized as CT $(d\rightarrow\pi^*)+L(\pi\rightarrow\pi^*)$.

The Region Around 33 kK. The observed strong band at 33.4 kK with a shoulder at 34.5 kK has been assigned to an internal ligand transition [37, 15] shifted to lower energy in comparison with the free ligand. According to the present calculation these bands are clearly due to $11\,^1E$ (37.5 kK) and $6\,^1A_2$ (37.9 kK). Calculations for planar bipyridyl *(trans)*, with the same carbon and nitrogen parameters as used in the present study, give the lowest $\pi-\pi^*$ transition at 38.8 kK (Table 12). The MO calculation of the iron complex thus gives two transitions "shifted" to lower energy compared with the lowest $\pi-\pi^*$ transition of bipyridyl. But $11\,^1E$ and $6\,^1A_2$ cannot be classified as internal ligand transitions. They both have some $d-\pi^*$ character, transferring 0.70 resp. 0.36 electrons from iron d orbitals to the ligand π system.

The Region Around 40 kK. The observed band at 40.5 kK, with a shoulder on the low energy side at 38.6 kK and a shoulder on the high energy side at 42.0 kK has previously been considered as due to the second $\pi-\pi^*$ transition in bipyridyl

[37]. In this region the present calculation gives one strong transition, $8\,^1A_2$, surrounded by two weaker transitions, $14\,^1E$ and $15\,^1E$. The low energy shoulder may be assigned to $7\,^1A_2$ and $13\,^1E$. All of these five states can be classified as CT $(d\rightarrow\pi^*)+L(\pi\rightarrow\pi^*)$ states with an electron transfer of about 0.3–0.4.

The Region in Far UV. Observations have not been extended further than 48 kK. They show a region with increasing intensity from 43.5 kK (Table 10). The calculations give two strong transitions, $12\,^1A_2$ (54.3 kK) and $24\,^1E$ (55.8 kK), classified as transitions within the π-system of the bipyridyl molecules. The calculated spectral pattern for $[Fe(II)\text{–}(bipy)_3]^{++}$ in this region resembles the one for *cis*-bipyridyl, as can be seen from Tables 10 and 12. For bipyridyl in cyclohexane solution there is an observed strong band at 52.4 kK (Table 12).

The Region Below 20 kK. The lower singlet and triplet transitions are given in Table 11. Palmer and Piper [38] observed in crystal spectra a weak band at 11.5 kK polarized perpendicular to the threefold z-axis. They assigned it as a spinforbidden $d-d$ transition ($^1A_1-{}^3T_1$ in O_h) gaining intensity through spin-orbit coupling with the visible CT band around 19 kK. They further attributed a weak sharp peak at 8.89 kK to the second overtone of the C–H stretching vibration. König and Schläfer [39] made a different assignment of the corresponding peak at 8.98 kK in solution spectra. They considered it to be a $^1A_1-{}^3T_1(O_h)$ d–d transition. According to the present calculation there are no d–d singlets or triplets in this low energy region. The observed band at 11.5 kK in crystal spectra [38] and 11.8 kK in solution spectra (Table 11) can most probably be assigned to the weak perpendicularly polarized $1\,^1E$ transition. According to the present calculations the tail of the observed strong band at 19.2 kK may be constituted of two weak singlets, $1\,^1E$ and $1\,^1A_2$, and three triplets, $1\,^3A_2$, $2\,^3E$ and $3\,^3E$.

Two low-lying triplets, $1\,^3A_1$ and $1\,^3E$, are predicted. Both or one of them may be attributed to the 8.85 kK peak, but it should be stressed that as yet there exist no clear experimental evidence for them. They might be revealed in luminescence spectra or by the aid of ESR measurements.

8. Conclusions

The method used in the present calculations had previously been applied in studies of organic copper complexes [4–7] and proven to be capable of giving a quantitative account for many different properties depending on the electronic structure. The present investigation shows that the method is also well suited for studies of iron organic compounds. The scheme for evaluation of one-center iron parameters and parameters describing the iron-ligand bond can of course be extended to other transition elements.

The results can be summarized as follows: For both $[Fe(II)\text{–}(GMI)_3]^{++}$ and $[Fe(II)\text{–}(bipy)_3]^{++}$ the calculated electronic population of the iron is in accord with Mössbauer isomer shift data, indicating that a realistic electron distribution has been obtained for the normal state. The electronic spectra of both compounds are quantitatively analyzed. Ligand field, charge transfer, and intraligand transitions are treated simultaneously and the interaction between them is properly taken into account. The method makes it possible to explain detailed properties

of the electronic spectra, e.g. the difference in intensity for the visible band in the neighbourhood of 29 kK in the two similar compounds.

Previous assignments based on O_h symmetry and crystal field theory can only be expected to give a rough qualitative picture of the spectral pattern, as trigonal distortion and covalency have been neglected. It is thus not astonishing that the present assignments for some bands differ considerably from previous conventional assignments.

For both compounds triplet $[CT(d \rightarrow \pi^*) + L(\pi - \pi^*)]$ states are predicted to be found in the near IR. The experimental verification of these bands remains to be done.

Appendix

One-Center Parameters for Iron from Observed Atomic Spectra and Atomic Analytical Hartree-Fock Wave Functions

In a semiempirical method considering the valence electrons (3*d*, 4*s* and 4*p*) of the transition metal ion, it would be desirable to obtain from experimental data the numerical values of the metal one-center parameters for different electronic populations and charges of the ion. Atomic spectral data can be used for the determination of the two-electron Slater-Condon parameters, $F_k(\mu, \nu)$, $G_k(\mu, \nu)$, and the one-electron parameters ε_μ (Eq. 6, Section 4). This is so because the energy of a spectroscopic term of an atom can be expressed in terms of these parameters [40–42]. With the assumption of a "frozen core" the energy is given by the expression:

$$E^{i,g} = C + \sum_{\mu} a^g(\mu)\varepsilon_\mu + \sum_{\mu>\nu}\sum \Big\{ b^g(\mu,\nu) F_0(\mu,\nu) + \sum_{k\neq 0} [c_k^{i,g}(\mu,\nu) F_k(\mu,\nu) - d_k^{i,g}(\mu,\nu) G_k(\mu,\nu)] \Big\} \tag{15}$$

where C is a constant particular to the element, μ and ν denote atomic valence orbitals, and i detones the i^{th} term of the configuration g.

Hinze and Jaffé [42] in an extensive study of the first transition elements using atomic term energies determined the Slater-Condon parameters with $k \neq 0$ for the neutral atom and the monopositive ion. Later Tondello *et al.* [43] using certain theoretical conditions together with spectral data made a new determination of the Slater-Condon parameters ($k \neq 0$) assuming the parameters to be charge dependent. Because of the lack of enough experimental information, it will not be possible to deduce from observed data only, the charge and configuration dependence of all one-center parameters needed in semiempirical calculations. Some extra assumptions have to be made.

In the present work a procedure for obtaining $F_k(\mu, \nu)$, $G_k(\mu, \nu)$ (including $k = 0$) and ε_μ for iron is presented. Atomic spectral data [44] are used in combination with some relations between theoretical Slater-Condon parameters, obtained from atomic analytical Hartree-Fock wave functions [25, 26, 45]. Recently a different approach was given by Anno and Teruya [46] in an elaborate study of the Slater-Condon parameters of all first transition elements.

The experimental spectroscopic energy of a multiplet was determined from Moore's tables [44] as a weighted mean of the J states. The following configurations and multiplets were considered.

d^8 : ^3F
d^7s : ^5F, ^5P, ^3H, ^1H, ^3G, ^1G
d^6s^2 : ^5D, ^3H, ^3G, ^3D, ^1I
d^7p : ^5F, ^5G, ^5S, ^5P, ^3I, ^1I
d^6sp: ^7D, ^7F, ^7P

d^7 : ^4F, ^4P, ^2G, ^2H, ^2F
d^6s : ^6D, ^4H, ^4G, ^2H, ^2I
d^5s^2 : ^6S, ^4D
d^6p : ^6D, ^6F, ^6P, ^4I, ^2K
d^5sp: ^8P

d^6 : ^5D, ^3H, ^3G, ^3D, ^1I, $^3\overline{F}$, ^1F, $^1\overline{G}$
d^5s : ^7S, ^5S, ^5G, ^5D, ^5F, ^3H, ^1H
d^5p : ^7P, ^5H, ^3K, ^1K.

For $^3\overline{F}$ and $^1\overline{G}$ in the configuration d^6, an average over two multiplets was used.

$F_k(\mu, \nu)$ *and* $G_k(\mu, \nu)$ *for* $k \neq 0$

The parameters $F_2(d, d)$, $F_4(d, d)$ and $G_2(s, d)$ were determined in the classical manner by a least-squares procedure from term energies for each considered configuration not containing $4p$. Different values for different configurations were obtained. An analysis of these values shows that $F_2(d, d)$ and $F_4(d, d)$ depend strongly and almost linearly on the number of $3d$-electrons (n_{3d}) and weakly on n_{4s}. Thus $F_2(d, d)$ and $F_4(d, d)$ are assumed to be linear functions of n_{3d} and a least-squares procedure gives:

$$F_2(d, d) = 1.418 - 0.171\,(n_{3d} - 6) \text{ in kK}, \tag{16}$$

$$F_4(d, d) = 0.114 - 0.009\,(n_{3d} - 6) \text{ in kK}. \tag{17}$$

It is also reasonable to describe $G_2(s, d)$ as a linear function of the charge, q.

$$G_2(s, d) = 1.290 + 0.269\,q \text{ in kK}. \tag{18}$$

The values of $F_2(d, d)$, $F_4(d, d)$ and $G_2(s, d)$ determined from Eqs. (16), (17) and (18) were then used in the expressions for the term energies in configurations with $4p$. Different values of $F_2(p, d)$ and $G_3(p, d)$ for different configurations were obtained. (No value of $F_2(p, d)$ could be determined for d^5p.)

$G_3(p, d)$ can be described as a linear function of q:

$$G_3(p, d) = 0.0162 + 0.0077\,q \text{ in kK}. \tag{19}$$

As there are not enough experimental spectroscopic data to allow for an analysis of the configuration dependence of $F_2(p, d)$, a comparison was made with theoretical values of this parameter. The theoretical data indicates that $F_2(p, d)$ is non-linearly q-dependent. In Table 1 the values of $F_2(p, d)$ for $q = 0$ and $q = 1$ are the experimentally derived values; the value for $q = 2$ is a "scaled" theoretical value,

where the scaling factor is the average quotient between experimental and theoretical values for $q = 0$ and 1.

As $G_1(p, d)$ could not be determined from the observed term energies, used in the present investigation, the values of this parameter are determined as:

$$G_1^e(p, d) = \left[\frac{G_1^t(p, d)}{G_3^t(p, d)}\right]_{\text{average value}} \cdot G_3^e(p, d) \tag{20}$$

where the index e stands for experimental and t for theoretical. As the quotient between $G_1^t(p, d)$ and $G_3^t(p, d)$ is found to be almost constant for different configurations, an average value of the quotient is used. It was not possible to determine $G_1(s, p)$ from the term energies considered, as it always occurs in the combination:

$$F_0'(s, p) = [F_0(s, p) - G_1(s, p)] . \tag{21}$$

ε_μ and $F_0(\mu, \nu)$

The parameters ε_μ and $F_0(\mu, \nu)$ ($F_0'(s, p)$ replacing $F_0(s, p)$) cannot be determined from term energies of just one configuration. "Average" values, over different ionic states and configurations, for these parameters, were derived from expressions of the barycenter energies of each configuration considered.

The values of $F_k(\mu, \nu)$ and $G_k(\mu, \nu)$ for $k \neq 0$, derived in the manner described above, were inserted in the expressions for the barycenter energies, giving linear equations for ε_μ and $F_0(\mu, \nu)$. The "average" values, $\bar{\varepsilon}_\mu$ and $\bar{F}_0(\mu, \nu)$ were determined from a least-squares fit to the equations thus obtained.

Theoretical values of $F_0^t(\mu, \nu)$ were calculated and corresponding average values, $\bar{F}_0^t(\mu, \nu)$ derived. An analysis of theoretical $F_0^t(\mu, \nu)$ values was made. It turned out that $F_0^t(d, d)$ with rather good accuracy can be described as a linear function of n_{3d}, while $F_0^t(s, s)$, $F_0^t(s, p)$, $F_0^t(s, d)$ and $F_0^t(p, d)$ can be considered as non-linear functions of q. This simplified population dependence of the theoretical F_0^t values is transformed to the semiempirical parameters by the formula:

$$F_0^e(\mu, \nu) = \left[\frac{\bar{F}_0^e(\mu, \nu)}{\bar{F}_0^t(\mu, \nu)}\right] \cdot F_0^t(\mu, \nu) . \tag{22}$$

The obtained values of $F_0^e(\mu, \nu)$ (see Table 1) were then inserted in the expressions for the barycenter energies of each configuration, giving linear equations for ε_μ. These equations can be solved assuming ε_{3d} to be a function of n_{3d}, and ε_{4s} and ε_{4p} to be functions of q. These assumptions are in line with the results for $F_k(\mu, \nu)$. The obtained semiempirical values of the one-center parameters are presented in Table 1. The values of $G_1^e(s, p)$ and $F_0^e(s, p)$, given in Table 1, are obtained from the values of $F_0'^e(s, p)$ assuming $[G_1^e(s, p)/F_0^e(s, p)]$ equal to the average theoretical value of $[G_1^t(s, p)/F_0^t(s, p)]$. $F_0(p, p)$ and $F_2(p, p)$ cannot be derived from experimental data. The values given in Table 1 have been roughly estimated as:

$$F_0^e(p, p) = 2F_0^e(s, p) - F_0^e(s, s) , \tag{23}$$

$$F_2^e(p, p) = \left[\frac{F_2^t(p, p)}{F_0^t(p, p)}\right]_{\text{average value}} \cdot F_0^e(p, p) . \tag{24}$$

The semiempirical parameters obtained are found to reproduce the spectroscopic energy terms of Fe in different ionic states with a standard deviation of 1.63 kK.

The present procedure can be considered as a method to "scale" theoretical parameter values in those cases where a direct determination from experimental data is not possible. The values in Table 1 must be looked upon as "a first trial" to these important parameters. New experimental data in combination with wave functions accounting for correlation (and eventually relativistic effects) will probably allow for a more detailed description of the configuration dependence of the parameters. A similar procedure can of course be used in a systematic study of all transition elements.

Acknowledgement. This investigation has been supported by grants from the Swedish Natural Science Research Council. The authors wish to express gratitude to Prof. Inga Fischer-Hjalmars for her encouraging interest throughout the work and also to Dr. Björn Roos for valuable discussions. Thanks are also due to Mr. Lars Norén for assistance in numerical computations.

References

1. Fischer-Hjalmars, I., Sundbom, M.: Acta chem. scand. **22**, 607 (1968).
2. Sundbom, M.: Acta chem. scand. **22**, 1317 (1968).
3. Sundbom, M.: Acta chem. scand. **25**, 487 (1971).
4. Roos, B.: Acta chem. scand. **20**, 1673 (1966).
5. Roos, B.: Acta chem. scand. **21**, 1855 (1967).
6. Roos, B.: Svensk kem. Tidskr. **80**, 204 (1968).
7. Roos, B., Sundbom, M.: J. molecular Spectroscopy **36**, 8 (1970).
8. McWhinnie, W. R., Miller, J. D.: Advances inorg. Chem. Radiochem. **12**, 135 (1969).
9. Krumholz, P.: Structure and Bonding **9**, 139 (1971).
10. Day, P., Sanders, N.: J. chem. Soc. (A), 1530 (1967).
11. Day, P., Sanders, N.: J. chem. Soc. (A), 1536 (1967).
12. Mulliken, R. S.: J. Amer. chem. Soc. **72**, 600 (1950); **74**, 811 (1952).
13. Murrell, J. N.: Quart. Rev. **15**, 191 (1961).
14. Ito, T., Tanaka, N., Hanazaki, I., Nagakura, S.: a) Bull. chem. Soc. Japan **41**, 365 (1968). b) Sci. Rep. Tohoku Univ., Ser. I, **50**, 168 (1967).
15. Hanazaki, I., Nagakura, S.: Inorg. Chemistry **8**, 648 (1969).
16. Hanazaki, I., Hanazaki, F., Nagakura, S.: J. chem. Physics **50**, 265 (1969).
17. Jaeger, F. M., van Dijk, J. A.: Z. anorg. allg. Chem. **227**, 273 (1936).
18. Krumholz, P.: J. Amer. chem. Soc. **75**, 2163 (1953).
19. Roos, B., Skancke, P. N.: Acta chem. scand. **21**, 233 (1967).
20. Roothaan, C. C. J.: Rev. mod. Physics **32**, 179 (1960).
21. Roos, B.: Acta chem. scand. **19**, 1715 (1965).
22. Goeppert-Mayer, M., Sklar, A. L.: J. chem. Physics **6**, 645 (1938).
23. McClellan, A. L.: Tables of experimental dipole moments. San Fransisco: Freeman 1963.
24. Wolfsberg, M., Helmholtz, L.: J. chem. Physics **20**, 837 (1952).
25. Blomquist, J., Roos, B., Sundbom, M.: USIP Report 71-07. This report is available upon request from Dr. Jan Blomquist, Inst. of Physics, University of Stockholm, Vanadisvägen 9, 11346 Stockholm.
26. Clementi, E.: IBM J. Res. Develop., Suppl. 9, 2 (1965).
27. Castellano, S., Günther, H., Ebersole, S.: J. physic. Chem. **69**, 4166 (1965).
28. Templeton, D. H., Zalkin, A., Ueki, T.: Acta crystallogr. **21**, A 154 (1966).
29. König, E., Watson, K. J.: Chem. Physics Letters **6**, 457 (1970).
30. Almenningen, A., Bastiansen, O.: Det Kgl. Nordiske Videnskabers Selskabs Skrifter 1958, Nr. 4.
31. Nordén, B., Håkansson, R., Sundbom, M.: Acta chem. scand. **26**, 429 (1972).
32. Hanazaki, I., Nagakura, S.: Inorg. Chemistry **8**, 654 (1969).
33. Blomquist, J., Roos, B., Sundbom, M.: J. chem. Physics **55**, 141 (1971).

34. Epstein, L. M.: J. chem. Physics **40**, 435 (1964).
35. König, E.: Coordin. Chem. Reviews **3**, 471 (1968).
36. Krumholz, P.: Structure and Bonding **9**, 139 (1971).
37. Bryant, G. M., Fergusson, J. E., Powell, H. K. J.: Austral. J. Chem. **24**, 257 (1971).
38. Palmer, R. A., Piper, T. S.: Inorg. Chemistry **5**, 864 (1966).
39. König, E., Schläfer, H. L.: Z. Physik. Chem. Neue Folge **34**, 355 (1962).
40. Slater, J. C.: Quantum theory of atomic structure, Vol. 1, Chapter 13. New York: McGraw-Hill Book Co. 1960.
41. Condon, E. U., Shortley, G. H.: The Theory of Atomic Structure, p. 174—183. New York: Cambridge University Press 1935.
42. Hinze, J., Jaffé, H. H.: J. chem. Physics **38**, 1834 (1963).
43. Tondello, E., de Michelis, G., Oleari, L., di Sipio, L.: Coord. Chem. Rev. **2**, 65 (1967).
44. Moore, C. E.: Circular of the National Bureau of Standards 467, Washington 1952.
45. Roos, B., Salez, C., Veillard, A., Clementi, E.: A General Program for Calculation of Atomic SCF Orbitals by the Expansion Method, Special IBM Technical Report, San José, California. IBM Research Laboratory 1968.
46. Anno, T., Teruya, H.: J. chem. Physics **52**, 2840 (1970).
47. Blomquist, J., Moberg, L.: USIP-Report 72-03, Jan. 1972.

Dr. M. Sundbom
Institute of Theoretical Physics
University of Stockholm
Vanadisvägen 9
11346, Stockholm, Sweden